

RESEARCH PAPER

## Rapid H<sub>2</sub>O<sub>2</sub>-Promoted Oxidation of Anazoline Sodium over the [BMIM]PF<sub>6</sub>/Pt/γ-Al<sub>2</sub>O<sub>3</sub> Nanocatalyst

Mohsen Padervand<sup>1,\*</sup>, Kaveh Gholami<sup>2</sup>, Hadi Salari<sup>3</sup>, Manouchehr Vosoughi<sup>4</sup>

<sup>1</sup> Faculty of Science, Department of Chemistry, University of Maragheh, Maragheh, Iran

<sup>2</sup> Department of Chemistry, University of Maragheh, Maragheh, Iran

<sup>3</sup> Department of Chemistry, College of Sciences, Shiraz University, Shiraz, Iran

<sup>4</sup> Institute for Biotechnology and Environment, Sharif University of Technology, Tehran, Iran

### ARTICLE INFO

#### Article History:

Received 08 February 2019

Accepted 18 May 2019

Published 01 July 2019

#### Keywords:

Anazoline Sodium

H<sub>2</sub>O<sub>2</sub>

Oxidation

γ-Al<sub>2</sub>O<sub>3</sub>

### ABSTRACT

Highly meso-porous Pt contained γ-Al<sub>2</sub>O<sub>3</sub> nanostructure was prepared by a combined sol gel-pyrolisis method in the presence of polyvinylpyrrolidone and Pluronic p123 as surfactant. The surface of the prepared nanostructure was decorated with 1-Butyl-3-methylimidazolium hexafluorophosphate ([BMM]PF<sub>6</sub>) ionic liquid to enhance the sorption capacity and prevent the poisoning of the catalytic active sites. The catalyst was characterized by X-ray diffraction powder (XRD), Transmission Electron Microscopy (TEM), Energy Dispersive X-ray (EDX), and Brunauer–Emmett–Teller surface analysis (BET) methods. The XRD pattern and the results of elemental analysis well confirmed the crystalline phase of gamma-alumina and the presence of Pt nanoparticles on the surface. Decolorization of Anazoline Sodium (AS) dye compound as a typical wastewater was carried out using H<sub>2</sub>O<sub>2</sub> as oxidative agent and the results showed that the prepared nanostructure had promising catalytic activity. The results of the recycling experiments showed that [BMIM]PF<sub>6</sub>/Pt/γ-Al<sub>2</sub>O<sub>3</sub> is more promising than Pt/γ-Al<sub>2</sub>O<sub>3</sub> which points out the role of ionic liquid layer on the surface.

#### How to cite this article

Padervand M, Gholami K, Salari H, Vosoughi M. Rapid H<sub>2</sub>O<sub>2</sub>-Promoted Oxidation of Anazoline Sodium over the [BMIM]PF<sub>6</sub>/Pt/γ-Al<sub>2</sub>O<sub>3</sub> Nanocatalyst. J Nanostruct, 2019; 9(3): 489-497. DOI: 10.22052/JNS.2019.03.010

### INTRODUCTION

Highly nanoporous metal oxides with accessible three-dimensional surface areas offer unprecedented opportunities in catalysis, energy technologies, environmental remediation, etc [1-4].

Al<sub>2</sub>O<sub>3</sub> has attracted great interest in variety of applications due to interesting catalytic, adsorption, optical, and electronic properties; so, the control and improvement of its physical-chemical characteristics is the key subject of ongoing studies [3-5]. Specifically, mesoporous Al<sub>2</sub>O<sub>3</sub> (MA) with unique channels, high surface area, and narrow pore-size distribution is highly desirable for many of industrial and academic usages [6, 7]. A substantial point to achieve the

ordered MA structures is solvent evaporation induced self-assembly (EISA) through various synthesis methods which all are mainly based on the sol-gel self assembly processes in the presence of soft (cationic, anionic, and nonionic surfactants) and hard (polymers and carbon molds) templates [6-9]. This allows fine-tuning of the structural properties of the MA-supported structures [10, 11]. Among its various crystalline phases, γ-Al<sub>2</sub>O<sub>3</sub> is the mostly used catalytic support in the automotive and petroleum industries. Surface chemical composition, thermal stability, phase composition, and its local microstructure lead to special acid/base characteristics in γ-alumina [12].

γ-Alumina has been extensively used to prepare efficient supported noble metal (Pt, Au, Pd, etc) and

\* Corresponding Author Email: [mohsenpadervand@gmail.com](mailto:mohsenpadervand@gmail.com)  
[padervand@maragheh.ac.ir](mailto:padervand@maragheh.ac.ir)

transition metal (Ni, Co, Fe, etc) catalysts [13-17]. A large number of papers have been discussing the catalytic properties of such materials to promote the dehydrogenation and common oxidation reactions [18-20]. Among the transition and noble metals for being used on the surface, nickel and platinum are the commonly used active agents [21]. Nickel is much cheaper but platinum is much more selective to catalyze the dehydrogenation at low and cracking reactions at high temperatures. According to the reports, the catalytic activity of the deposited Pt nanoparticles is incredibly affected by the microstructure of the support [21, 22]. To clarify this point, various organic and inorganic materials such as silica [23], activated carbon [24], carbon nanotubes [25], nanofibers [26], zirconia [27], metal organic frameworks (MOFs) [28], aluminas [14, 17, 29], zeolites [30], etc have been investigated and the results confirmed that  $\gamma$ -alumina can be selected as a promising candidate to be used in practical applications.

Because of unique properties including negligible vapor pressures, good electric conductivity, high thermal stability, high solvation interactions with both polar and non-polar compounds, and wide liquid temperature ranges and electrochemical windows, Room Temperature Ionic Liquids (RTILs) have attracted much attention in the synthesis of highly selective structures with a wide range of industrial applications [31]. Besides, RTILs are

specifically useful for the preparation of different kinds of nanoparticles with well-controlled morphology, sizes, and shapes, due to their extremely low vapor pressure and capability of dissolving various types of substrates and uniformly-dispersing a variety of solid-like particles. It has been demonstrated that the deposition of noble metals such as Au, Ag, and Pt in RTILs included matrixes results in corresponding metal nanoparticles, easily dispersed in the solution without using any additional stabilizing agent [32].

Herein, we reports the preparation of Pt loaded  $\gamma$ -alumina nanostructures. Decorating the surface with the [BMIM]PF<sub>6</sub> ionic liquid layer was also performed to improve the sorption and catalytic activity. The prepared catalysts, well analyzed by XRD, TEM, EDX, and BET characterization methods, exhibited incredible catalytic activity toward oxidation of AS in the presence of hydrogen peroxide (Fig. 1). The experimental conditions are optimized to get the highest efficiency and a suitable mechanism was proposed for the oxidation reaction.

## MATERIALS AND METHODS

### Preparation of the catalyst

H<sub>2</sub>PtCl<sub>6</sub>·6H<sub>2</sub>O and Al(NO<sub>3</sub>)<sub>3</sub>·9H<sub>2</sub>O (0.001 mol) were dissolved in a solution (water/ethanol: 20/80) contained Pluronic P123 (1 g) and polyvinylpyrrolidone (PVP, 0.5 g). AlCl<sub>3</sub> (0.01 mol)

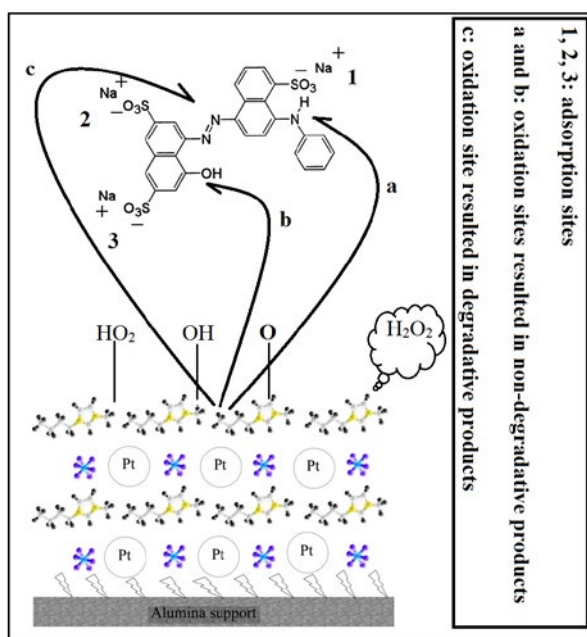


Fig. 1. H<sub>2</sub>O<sub>2</sub>-promoted catalytic oxidation of AS over the prepared nanostructures

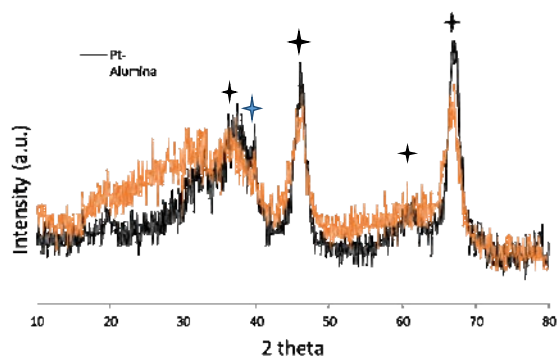


Fig. 2. The XRD patterns of the prepared structures

was added and the system was stirred at 50 °C for 3 h, aged for 12 h, and heated at 60 °C overnight to remove the solvent and obtain a xerogel. The product was heated at 550 °C for 5 h with a heating rate of 5 °C/min. The product (Pt/ $\gamma$ -Al<sub>2</sub>O<sub>3</sub>) was finely powdered and dispersed in a [BMIM]PF<sub>6</sub> (in acetonitrile) solution to decorate the surface with ionic liquid layer. After 2 h of stirring at room temperature, the precipitate collected, washed with distilled water and ethanol repeatedly, and dried at 70 °C overnight.

#### Catalytic oxidation of AS

The catalytic experiments were performed in a quartz reactor surrounded by a circulating water jacket (Pyrex) to keep the temperature of the reaction medium at 26 °C. The catalyst powder was dispersed in the AS solution and then, diluted hydrogen peroxide solution (2%) was injected. Sampling was done at different time intervals of the reaction and analyzed by a UV spectrophotometer adjusted at AS lambda max (574 nm).

## RESULTS AND DISCUSSION

### Catalyst characterization

XRD analysis was carried out to find the crystalline phase of the prepared structures and the results are indicated in Fig. 2. The characteristic peaks at 2theta 37.3, 46.0, 60.9 and 67.0° (black stars) are assigned to the Al<sub>2</sub>O<sub>3</sub> gamma phase.

Pt diffraction peak is also appeared at 39.5° (blue star) which is attributed to the growth of Pt (111) surface orientation [34]. The [BMIM]PF<sub>6</sub>/Pt/ $\gamma$ -Al<sub>2</sub>O<sub>3</sub> pattern was similar to that of Pt/ $\gamma$ -Al<sub>2</sub>O<sub>3</sub> with a decrease in intensity of Pt (111) characteristic peak which is due to the presence of [BMIM]PF<sub>6</sub> layer on the crystalline surfaces. TEM images of the prepared nanostructures are shown in Fig. 3 which confirms the presence of Pt nanoparticles in the

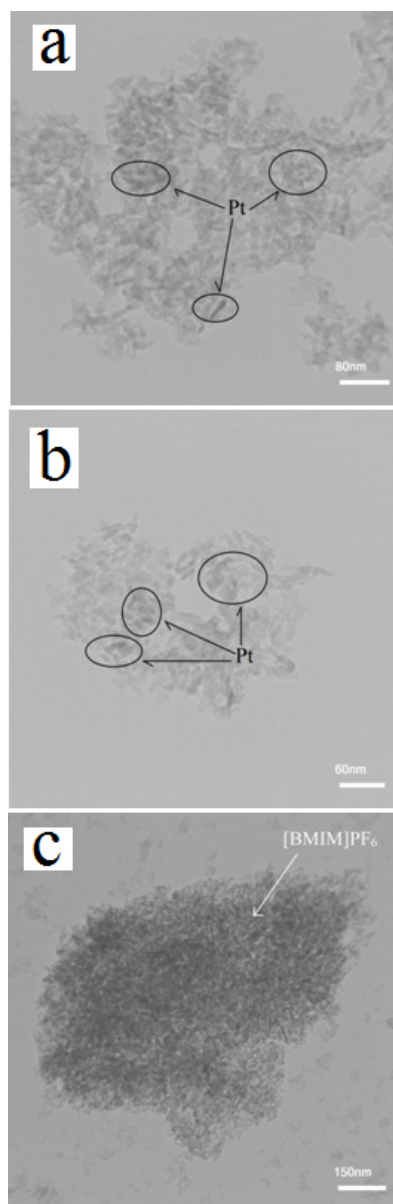
Fig. 3. TEM images of Pt/ $\gamma$ -Al<sub>2</sub>O<sub>3</sub> (a and b) and [BMIM]PF<sub>6</sub>/Pt/ $\gamma$ -Al<sub>2</sub>O<sub>3</sub> (c)

Table 1. The elemental analysis of the prepared catalyst

Element	Line	K	Kr	W%	A%
O	Ka	0.4519	0.2476	56.18	69.09
Al	Ka	0.5294	0.2901	42.15	30.74
Pt	La	0.0187	0.0102	1.67	0.17
		1.0000	0.5479	100.00	100.00

chemical texture. TEM images well demonstrate the formation of ionic liquid layer on the surface of Pt/ $\gamma$ -Al<sub>2</sub>O<sub>3</sub>.

Furthermore, from Fig. 3, the average size of the catalytic agents is below 80 nm and it's not easy to allocate a specific regular shape to the Pt nanoparticles in the structure. EDX analysis was performed to find the elemental percentage and the results (Fig. 4 and Table 1) indicated that the prepared catalyst contained Pt, Al, and O as the main constituents.

Moreover, the amount of platinum in the chemical structure of the catalyst was as the same as the quantity used during the preparation steps (~2%). To find the specific surface area and pore size distribution, as important factors to control the catalytic activity, BET and BJH analyses were carried out and the results are represented in Fig. 5a and 4b. BET analysis evaluates specific surface area of materials by nitrogen multilayer adsorption measured as a function of relative pressure using a fully automated analyzer. The technique encompasses external area and pore area measurements to determine the total specific surface area in m<sup>2</sup>/g. BJH analysis is also employed to determine pore area and specific pore volume using adsorption and desorption techniques. This technique characterises pore size distribution independent of external area.

The hysteresis loop obtained from N<sub>2</sub> adsorption-

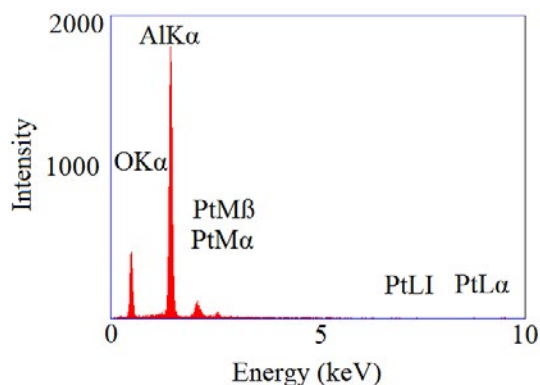


Fig. 4. The result of EDX analysis for the prepared catalyst PtM $\beta$

desorption isotherm well demonstrates the high porosity of the Pt/ $\gamma$ -Al<sub>2</sub>O<sub>3</sub> catalyst. According to this analysis, the specific surface area was determined to be 315 and 308 m<sup>2</sup>/g for Pt/ $\gamma$ -Al<sub>2</sub>O<sub>3</sub> and [BMIM]PF<sub>6</sub>/Pt/ $\gamma$ -Al<sub>2</sub>O<sub>3</sub>. Expected to be observed, the small decrease in surface area is due to the [BMIM]PF<sub>6</sub> layer on the surface which cover the pores and channels. Furthermore, from Fig. 5b, the maximum in pore size distribution curve is located between 2-50 nm and this indicates that the prepared catalyst is mesoporous.

#### Rapid oxidation of AS over the prepared catalysts

As a control experiment, 1 mL of H<sub>2</sub>O<sub>2</sub> (2%) solution was added to 50 mL of AS solution (20 ppm) and kept at room temperature to evaluate

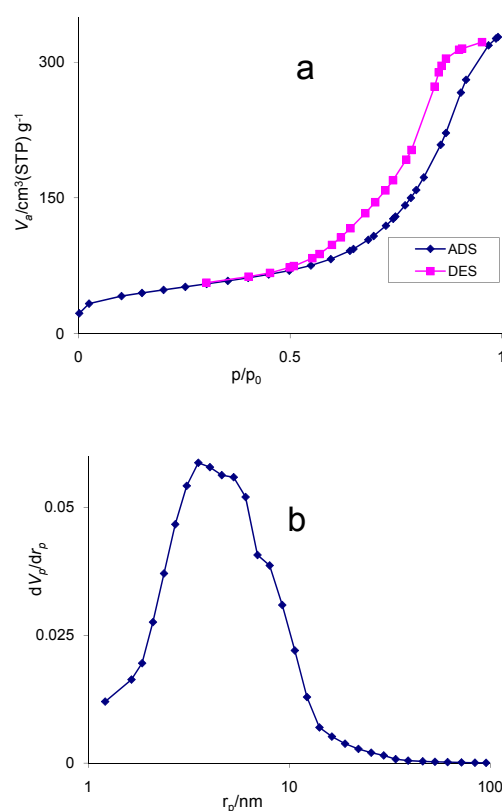


Fig. 5. Nitrogen adsorption-desorption isotherm (a) and the pore size distribution curve (b) of the prepared catalyst

the likely reactivity of the compounds in the absence of the prepared structures. After 72 h, the solution didn't show significant decrease in concentration (lower than 2%) and this convinced us to use of the prepared nanostructure to catalyze the reaction. The experiments were performed with different concentrations of AS and catalyst and the results are indicated in Fig. 6a and 6b.

According to Fig. 6, the reaction efficiency enhanced impressively by increasing the catalyst dosage up to 10 mg and then became constant. This typically reminds the needed effective number of catalytic active sites to promote the oxidation reaction on the surface while the further quantities just provide more sorption sites in the medium. Changing the AS concentration had the same effect and we found that 40 ppm was

the best concentration. Occupying the most of catalytic active sites by AS organic molecules and interfering with the heterogeneous oxidation pathway on the surface, the higher concentrations of AS decreased the reaction efficiency. To initiate the catalytic oxidation reaction, approaching the substrate and oxidative agent to the surface of the catalyst must be occurred under an equilibrium condition. Out of such condition which is considerably controlled by the substrate concentration and catalyst dosage, the reaction efficiency decreases. H<sub>2</sub>O<sub>2</sub> concentration was also optimized to get the highest efficiency. From the results (Fig. 7), increasing the concentration up to 400 ppm increases the oxidation efficiency.

The reaction efficiency reached to more than 99 % within 10 min when H<sub>2</sub>O<sub>2</sub> concentration

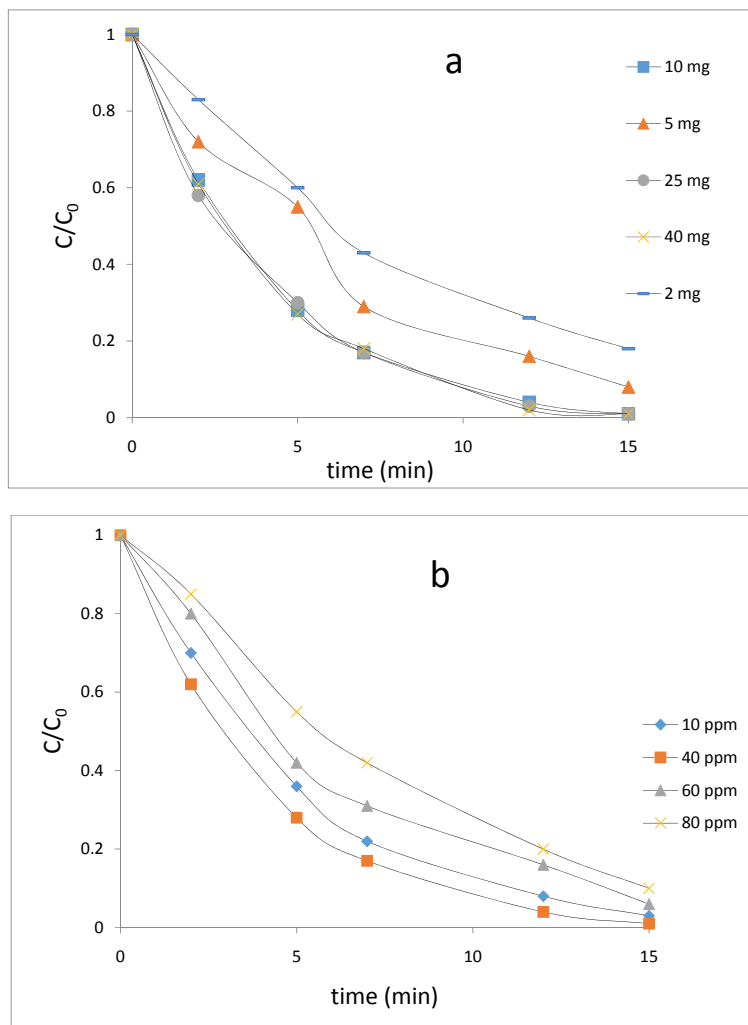


Fig. 6. The effect of catalyst dosage and AS concentration on the reaction efficiency

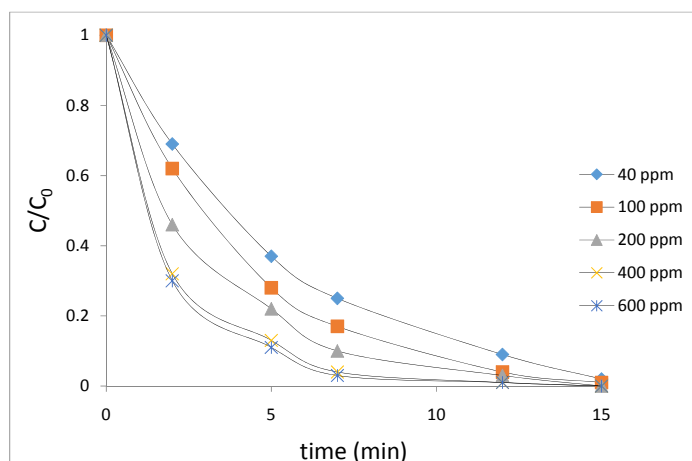


Fig. 7. The effect of hydrogen peroxide concentration on the AS oxidation reaction

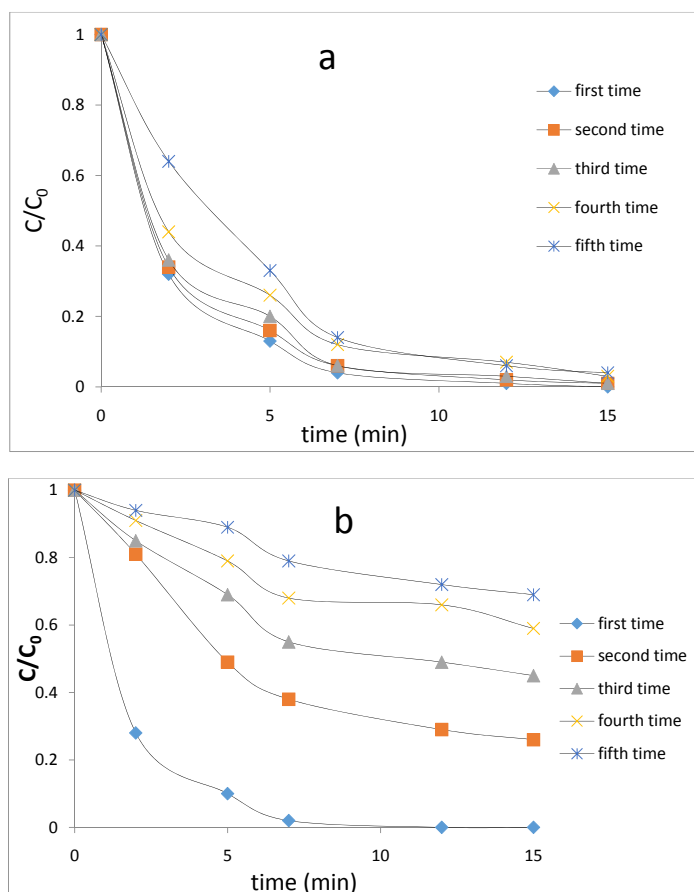


Fig. 8. The results of recycling experiments for the AS oxidation over the prepared catalyst (a: [BMIM]PF<sub>6</sub>/Pt/γ-Al<sub>2</sub>O<sub>3</sub> and b: Pt/γ-Al<sub>2</sub>O<sub>3</sub>)

increased from 40 to 400 ppm. This is assigned to the generation of a peroxy-intermediate and OH radicals attacking the organic molecules to oxidize them [35]. Introducing as promising candidate

for being used in the practical applications, the recycling experiments remarked the role of [BMIM]PF<sub>6</sub> layer on the surface of the prepared catalyst. From Fig. 8, [BMIM]PF<sub>6</sub>/Pt/γ-Al<sub>2</sub>O<sub>3</sub>

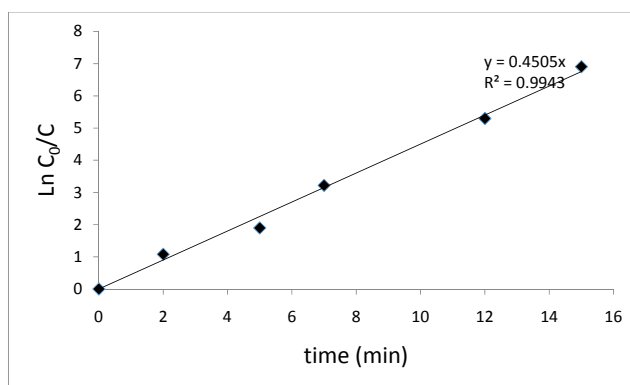
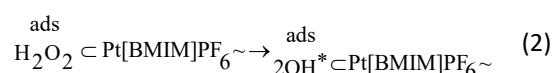
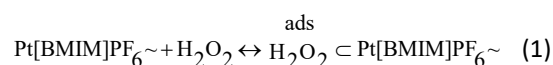


Fig. 9. Kinetic fit for the oxidation reaction of AS over the prepared catalyst

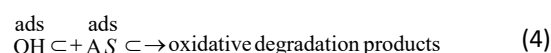
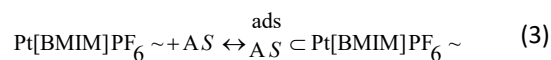
indicated much better capacity than Pt/γ-Al<sub>2</sub>O<sub>3</sub> during repeated using for AS oxidation. In fact, the catalytic active sites of Pt/γ-Al<sub>2</sub>O<sub>3</sub> particles were easily poisonous due to strong chemical sorption of anionic AS molecules onto the surface. [BMIM]PF<sub>6</sub> as a water insoluble ionic liquid, can control the chemical binding of water-solvated AS molecules to the surface of the catalytic particles. This reduces the poisoning of the catalytic active sites of the prepared nanostructure during the repeated uses. In addition, the cationic segment of the IL ([BMIM]<sup>+</sup>) can act as an absorptive part of the [BMIM]PF<sub>6</sub>/Pt/γ-Al<sub>2</sub>O<sub>3</sub> nanostructure to attract the sulfonate heads of the AS molecules while they are not strongly adsorbed on the surface in comparison with that of Pt/γ-Al<sub>2</sub>O<sub>3</sub>.

As can be seen, the catalytic activity of [BMIM]PF<sub>6</sub>/Pt/γ-Al<sub>2</sub>O<sub>3</sub> decreased smoothly after 6 times of repeated using. On the other hand, the reaction efficiency significantly descended for Pt/γ-Al<sub>2</sub>O<sub>3</sub> after second time of recycling. In addition, the experimental data demonstrated that the oxidation of AS over the prepared nanostructures followed first order kinetics which means that  $\ln A/A_0 = f(t)$  was expected to be linear. From Fig. 9, the rate constant for the reaction under the optimized conditions was determined to be 0.45 min<sup>-1</sup>.

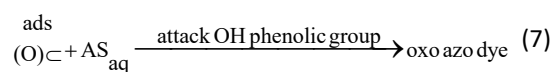
The theoretical-experimental results released by Lousada et al. confirmed that the H<sub>2</sub>O<sub>2</sub> promoted oxidation mechanism on the surface of suspended solids in aqueous solution includes the existence of an adsorption step [36].



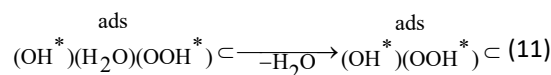
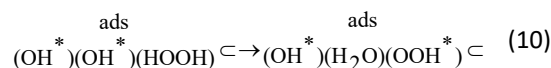
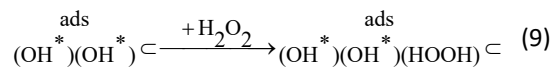
AS is also adsorbed on the surface and this can be demonstrated by the following equations:



OH radicals generated on the surface can also be converted to other oxidative species which promotes the oxidation reaction from a different pathway:



In addition to above oxidative species, HO<sub>2</sub> radicals are the other reactive agents produced from H<sub>2</sub>O<sub>2</sub> dissociation on the surface which act pretty slower than the former types.



The symbol  $\subset$  in the equations 1-11 is the symbol of “on the surface”. From the proposed mechanism, collisions between the reactants in both aqueous and particulate phases promote the oxidative mechanism and prevention of each step reduces the reaction efficiency significantly.

From the obtained results, it is obvious that the prepared catalyst is highly active to decolorize the AS solution and oxidize a typical dye compound below 15 min of the reaction time which was very faster than the similar reactions investigated by the previous researchers [37, 38].

## CONCLUSIONS

Mesoporous Pt loaded [BMIM] decorated  $\gamma$ -Al<sub>2</sub>O<sub>3</sub> nanostructures prepared by a sol gel-pyrolysis method using PVP and Pluronic p123 as surfactant and template agents. The results showed that the IL layer on the surface enhanced the sorption capacity and diminished the poisoning rate of catalytic active sites. XRD patterns and EDX analysis well confirmed the presence of Pt (111) nanoparticles on the surface of the support. BET and BJH analyses indicated that prepared catalyst was mesoporous with specific surface area of ~350 m<sup>2</sup>/g. The results of the H<sub>2</sub>O<sub>2</sub>-promoted catalytic experiments implied that the prepared catalyst were incredibly able to oxidize AS in the aqueous phase. 10 mg and 40 ppm were selected as the optimum values for catalyst dosage and AS concentration. According to the recycling experiments, [BMIM]PF<sub>6</sub>/Pt/ $\gamma$ -Al<sub>2</sub>O<sub>3</sub> exhibited a promising capacity after six times of repeated decolorization of the AS solutions and being used in the practical applications which points out the role of ionic liquid layer on the surface.

## CONFLICT OF INTEREST

The authors declare that there are no conflicts of interest regarding the publication of this manuscript.

## REFERENCES

- Sangsefidi FS, Salavati-Niasari M. Thermal decomposition synthesis, characterization and electrochemical hydrogen storage characteristics of Co<sub>3</sub>O<sub>4</sub>-CeO<sub>2</sub> porous nanocomposite. *International Journal of Hydrogen Energy*. 2017;42(31):20071-81.
- Sangsefidi FS, Salavati-Niasari M, Shabani-Nooshabadi M. Characterization of hydrogen storage behavior of the as-synthesized p-type NiO/n-type CeO<sub>2</sub> nanocomposites by carbohydrates as a capping agent: The influence of morphology. *International Journal of Hydrogen Energy*. 2018;43(31):14557-68.
- Trueba M, Trasatti SP.  $\gamma$ -Alumina as a Support for Catalysts: A Review of Fundamental Aspects. *European Journal of Inorganic Chemistry*. 2005;2005(17):3393-403.
- Márquez-Alvarez C, Žilková N, Pérez-Pariente J, Čejka J. Synthesis, Characterization and Catalytic Applications of Organized Mesoporous Aluminas. *Catalysis Reviews*. 2008;50(2):222-86.
- Cai W, Yu J, Cheng B, Su B-L, Jaroniec M. Synthesis of Boehmite Hollow Core/Shell and Hollow Microspheres via Sodium Tartrate-Mediated Phase Transformation and Their Enhanced Adsorption Performance in Water Treatment. *The Journal of Physical Chemistry C*. 2009;113(33):14739-46.
- Cai W, Yu J, Mann S. Template-free hydrothermal fabrication of hierarchically organized  $\gamma$ -AlOOH hollow microspheres. *Microporous and Mesoporous Materials*. 2009;122(1-3):42-7.
- Yu X, Yu J, Cheng B, Jaroniec M. Synthesis of Hierarchical Flower-like AlOOH and TiO<sub>2</sub>/AlOOH Superstructures and their Enhanced Photocatalytic Properties. *The Journal of Physical Chemistry C*. 2009;113(40):17527-35.
- Cai W, Yu J, Gu S, Jaroniec M. Facile Hydrothermal Synthesis of Hierarchical Boehmite: Sulfate-Mediated Transformation from Nanoflakes to Hollow Microspheres. *Crystal Growth & Design*. 2010;10(9):3977-82.
- Bejenaru N, Lancelot C, Blanchard P, Lamonier C, Rouleau Lc, Payen E, et al. Synthesis, Characterization, and Catalytic Performances of Novel CoMo Hydrodesulfurization Catalysts Supported on Mesoporous Aluminas. *Chemistry of Materials*. 2009;21(3):522-33.
- Zhang Z, Pinnavaia TJ. Mesoporous  $\gamma$ -Alumina Formed Through the Surfactant-Mediated Scaffolding of Peptized Pseudoboehmite Nanoparticles. *Langmuir*. 2010;26(12):10063-7.
- Dong A, Ren N, Tang Y, Wang Y, Zhang Y, Hua W, et al. General Synthesis of Mesoporous Spheres of Metal Oxides and Phosphates. *Journal of the American Chemical Society*. 2003;125(17):4976-7.
- Sun Y, Wang H, Li P, Geng H, Xu J, Han Y. Effects of the Facet Orientation of  $\gamma$ -Al<sub>2</sub>O<sub>3</sub> Support on the Direct Synthesis of H<sub>2</sub>O<sub>2</sub> Catalyzed by Pd Nanoparticles. *European Journal of Inorganic Chemistry*. 2018;2018(16):1715-25.
- Alexeev OS, Chin SY, Engelhard MH, Ortiz-Soto L, Amiridis MD. Effects of Reduction Temperature and Metal-Support Interactions on the Catalytic Activity of Pt/ $\gamma$ -Al<sub>2</sub>O<sub>3</sub> and Pt/TiO<sub>2</sub> for the Oxidation of CO in the Presence and Absence of H<sub>2</sub>. *The Journal of Physical Chemistry B*. 2005;109(49):23430-43.
- Liu L, Zhou F, Wang L, Qi X, Shi F, Deng Y. Low-temperature CO oxidation over supported Pt, Pd catalysts: Particular role of FeOx support for oxygen supply during reactions. *Journal of Catalysis*. 2010;274(1):1-10.
- Lin C-H, Chen C-L, Wang J-H. Mechanistic Studies of Water-Gas-Shift Reaction on Transition Metals. *The Journal of Physical Chemistry C*. 2011;115(38):18582-8.
- Garbarino G, Riani P, Magistri L, Busca G. A study of the methanation of carbon dioxide on Ni/Al<sub>2</sub>O<sub>3</sub> catalysts at atmospheric pressure. *International Journal of Hydrogen Energy*. 2014;39(22):11557-65.
- He S, Sun C, Bai Z, Dai X, Wang B. Dehydrogenation of long chain paraffins over supported Pt-Sn-K/Al<sub>2</sub>O<sub>3</sub> catalysts: A study of the alumina support effect. *Applied Catalysis A: General*. 2009;356(1):88-98.
- García-Diéguez M, Finocchio E, Larrubia MÁ, Alemany LJ,

- Busca G. Characterization of alumina-supported Pt, Ni and PtNi alloy catalysts for the dry reforming of methane. *Journal of Catalysis*. 2010;274(1):11-20.
19. Kousi K, Kondarides DI, Verykios XE, Papadopoulou C. Glycerol steam reforming over modified Ru/Al<sub>2</sub>O<sub>3</sub> catalysts. *Applied Catalysis A: General*. 2017;542:201-11.
20. Bilal M, Jackson SD. Ethanol steam reforming over Pt/Al<sub>2</sub>O<sub>3</sub> and Rh/Al<sub>2</sub>O<sub>3</sub> catalysts: The effect of impurities on selectivity and catalyst deactivation. *Applied Catalysis A: General*. 2017;529:98-107.
21. Ballarini AD, Zgolicz P, Vilella IMJ, de Miguel SR, Castro AA, Scelza OA. n-Butane dehydrogenation on Pt, PtSn and PtGe supported on  $\gamma$ -Al<sub>2</sub>O<sub>3</sub> deposited on spheres of  $\alpha$ -Al<sub>2</sub>O<sub>3</sub> by washcoating. *Applied Catalysis A: General*. 2010;381(1-2):83-91.
22. Okada Y, Sasaki E, Watanabe E, Hyodo S, Nishijima H. Development of dehydrogenation catalyst for hydrogen generation in organic chemical hydride method. *International Journal of Hydrogen Energy*. 2006;31(10):1348-56.
23. Akamatsu K, Ohta Y, Sugawara T, Hattori T, Nakao S-i. Production of Hydrogen by Dehydrogenation of Cyclohexane in High-Pressure (1–8 atm) Membrane Reactors Using Amorphous Silica Membranes with Controlled Pore Sizes. *Industrial & Engineering Chemistry Research*. 2008;47(24):9842-7.
24. Sebastián D, Bordejé EG, Calvillo L, Lázaro MJ, Moliner R. Hydrogen storage by decalin dehydrogenation/naphthalene hydrogenation pair over platinum catalysts supported on activated carbon. *International Journal of Hydrogen Energy*. 2008;33(4):1329-34.
25. Wang Y, Shah N, Huggins FE, Huffman GP. Hydrogen Production by Catalytic Dehydrogenation of Tetralin and Decalin Over Stacked Cone Carbon Nanotube-Supported Pt Catalysts. *Energy & Fuels*. 2006;20(6):2612-5.
26. Tien PD, Satoh T, Miura M, Nomura M. Continuous hydrogen evolution from cyclohexane over platinum catalysts supported on activated carbon fibers. *Fuel Processing Technology*. 2008;89(4):415-8.
27. Wang B, Froment G, Goodman D. CO-free hydrogen production via dehydrogenation of a Jet A hydrocarbon mixture. *Journal of Catalysis*. 2008;253(2):239-43.
28. Dai C, Liu F, Zhang W, Li Y, Zhang C. Deactivation study of Pd/Al<sub>2</sub>O<sub>3</sub> catalyst for hydrogenation of benzonitrile in fixed-bed reactor. *Appl. Catal. A Gen*, 2017; 538: 199–206.
29. Yolcular S, Olgun Ö. Ni/Al<sub>2</sub>O<sub>3</sub> catalysts and their activity in dehydrogenation of methylcyclohexane for hydrogen production. *Catalysis Today*. 2008;138(3-4):198-202.
30. Liu S, Wu X, Luo H, Weng D, Ran R. Pt/Zeolite Catalysts for Soot Oxidation: Influence of Hydrothermal Aging. *The Journal of Physical Chemistry C*. 2015;119(30):17218-27.
31. Plechkova NV, Seddon KR. Applications of ionic liquids in the chemical industry. *Chem Soc Rev*. 2008;37(1):123-50.
32. Fridman VZ, Xing R. Investigating the CrO<sub>x</sub>/Al<sub>2</sub>O<sub>3</sub> dehydrogenation catalyst model: II. Relative activity of the chromium species on the catalyst surface. *Applied Catalysis A: General*. 2017;530:154-65.
33. Anjaneyulu C, Costa LOO, Ribeiro MC, Rabelo-Neto RC, Noronha FB. Effect of Zn addition on the performance of Ni/Al<sub>2</sub>O<sub>3</sub> catalyst for steam reforming of ethanol. *Phys. Status Solidi. B*, 2016; 519: 85–98.
34. Gatel C, Baules P, Snoeck E. Morphology of Pt islands grown on MgO(001). *Journal of Crystal Growth*. 2003;252(1-3):424-32.
35. Dulman V, Cucu-Man SM, Olariu RI, Buhaceanu R, Dumitras M, Bunia I. A new heterogeneous catalytic system for decolorization and mineralization of Orange G acid dye based on hydrogen peroxide and a macroporous chelating polymer. *Dyes and Pigments*. 2012;95(1):79-88.
36. Lousada CM, Johansson AJ, Brinck T, Jonsson M. Mechanism of H<sub>2</sub>O<sub>2</sub> Decomposition on Transition Metal Oxide Surfaces. *The Journal of Physical Chemistry C*. 2012;116(17):9533-43.
37. Fang Z-d, Zhang K, Liu J, Fan J-y, Zhao Z-w. Fenton-like oxidation of azo dye in aqueous solution using magnetic Fe<sub>3</sub>O<sub>4</sub>-MnO<sub>2</sub> nanocomposites as catalysts. *Water Science and Engineering*. 2017;10(4):326-33.
38. Hua L, Ma H, Zhang L. Degradation process analysis of the azo dyes by catalytic wet air oxidation with catalyst CuO/ $\gamma$ -Al<sub>2</sub>O<sub>3</sub>. *Chemosphere*. 2013;90(2):143-9.